

Original article

Anatomical correlation of the helical structure of the ventricular myocardium through echocardiography



Omar Yassef Antúnez Montes

Escuela Superior de Medicina, Instituto Politécnico Nacional, Mexico City, Mexico

Article history:

Received 24 July 2018

Accepted 23 October 2018

Available online 15 April 2019

Keywords:

Myocardial band
Echocardiography
Myocardial dissection
Cardiac anatomy
Ventricular function
Cardiac physiology

Palabras clave:

Banda miocárdica
Ecocardiografía
Dissección del miocardio
Anatómica cardíaca
Función ventricular
Fisiología cardíaca

ABSTRACT

Introduction and objectives: The helical structure of the ventricular myocardium provides a simple view of cardiac anatomy, based on physiological evidence that has been broadly demonstrated in experimental and imaging studies, and helps to explain the electromechanical contraction of the myocardium during the cardiac cycle. The aim of this study was to standardize and provide a detailed description of the technique for preparing and manually dissecting the myocardium proposed empirically by Torrent-Guasp. A further aim was to anatomically and topographically correlate the helical band with echocardiographic long-axis, short-axis, and 4-chamber projections.

Methods: We dissected 42 hearts—20 bovine, 20 porcine and 2 human hearts—to standardize the myocardial dissection technique. Subsequently, the distinct segments were color coded to correlate the anatomical specimens with echocardiographic projections.

Results: Loss of 38% of the myocardial mass after boiling was sufficient to standardize myocardial dissection and allowed an efficient technique. No morphological differences were found between the bands of the hearts studied. The 4 myocardial segments could be identified in the echocardiographic projections.

Conclusions: Standardization of the technique is useful to dissect any type of heart. Echocardiography is useful to assess the distinct segments that compose the myocardium. More research is needed to generate practical applications of this knowledge to echocardiography and other fields.

© 2018 Sociedad Española de Cardiología. Published by Elsevier España, S.L.U. All rights reserved.

Correlación anatómica de la estructura helicoidal del miocardio ventricular mediante ecocardiografía

RESUMEN

Introducción y objetivos: La estructura helicoidal del miocardio ventricular ofrece una comprensión simple de la anatomía cardíaca bajo un argumento fisiológico demostrado en estudios experimentales y de imagen cardíaca que da sentido a la contracción electromecánica durante el ciclo cardíaco. Se ha estandarizado descriptivamente la técnica de preparación y disección del miocardio propuesta empíricamente por Torrent-Guasp mediante digitodisección para correlacionar anatómica y topográficamente la banda helicoidal con proyecciones ecocardiográficas de eje largo, eje corto y de 4 cámaras.

Métodos: Se disecaron 42 corazones —20 bovinos, 20 porcinos y 2 humanos— para estandarizar la técnica de disección del miocardio; después se identificaron con colores los diferentes segmentos para correlacionar las piezas anatómicas con las proyecciones ecocardiográficas.

Resultados: La pérdida del 38% de la masa estandariza la disección, y resulta eficiente para realizar la disección del miocardio. No se encontró diferencia morfológica en la banda de los corazones estudiados. En las proyecciones ecocardiográficas se pueden identificar los 4 segmentos miocárdicos.

Conclusiones: La estandarización de la técnica es útil para disecar cualquier tipo de corazón. El ecocardiograma es útil para valorar los diferentes segmentos en que se divide el miocardio. Se necesitan más estudios que generen otras aplicaciones prácticas de este conocimiento a la ecocardiografía y otros campos.

© 2018 Sociedad Española de Cardiología. Publicado por Elsevier España, S.L.U. Todos los derechos reservados.

Abbreviations

AS: ascending segment
 BL: basal loop
 DS: descending segment
 IVS: interventricular septum
 LS: left segment
 RS: right segment

INTRODUCTION

The helical structure of the ventricular myocardium as a single muscle band offers a simple understanding of the cardiac anatomy,¹ with physiologic evidence broadly demonstrated in experimental^{2,3} and imaging studies^{4,5} that helps explain the electromechanical contraction of the myocardium.

The ventricular myocardium is composed of 2 loops (basal loop [BL] and apical loop [AL]) and 4 segments (right [RS], left [LS], descending [DS], and ascending [AS]) that, rolled up over each other, define a band originating from the root of the pulmonary artery and ending at the aortic root⁶; one loop separates the other when the myocardium rotates 180°, forming an endocardial segment with descending fibers in the left ventricle (LV) that, once they reach the apex, change direction by means of a rotation to ascending epicardial fibers⁷ (Figure 1).

To anatomically correlate the band with echocardiographic views, we describe a standardized version of the dissection technique empirically proposed by Torrent-Guasp, in view of the difficulty involved in dissection. Objective dissection of hearts, regardless of species and size, allows the echographic views to be reproduced in the helical model.

The aim was to standardize and provide a detailed description of the technique for preparing and manually dissecting the myocardium that would show the helical structure of ventricles and to topographically correlate the position of the helical band and its segments with echocardiographic long-axis, short-axis, and 4-chamber views.

METHODS

The dissection was performed with an Adam Equipment AQ 2610S mechanical balance, dissection kit, 80% xylene, 100%



Figure 1. Unfolded myocardial band: human (A), bovine (B), and porcine (C). Blue: right segment; red: left segment; yellow: descending segment; green: ascending segment.

acetone, heat source for boiling, 20 bovine hearts, 20 porcine hearts, and 2 human hearts, all free of disease. The study was approved by the research ethics committee of the Venezuelan Society of Ultrasound in Obstetrics and Gynecology (SOVUOG), in compliance with the current regulations of the General Health Law of Mexico for the disposition and health control of organs and tissues.

Preparation of the Hearts

Bovine and Porcine Hearts

If the hearts have not undergone fixation, hydrocarbon immersion is not necessary, as unfixed adipose tissue is readily loosened by boiling.

Human Hearts

The human hearts were harvested from cadavers belonging to the School of Medicine at the Instituto Politécnico Nacional, previously fixed in 10% formol. The organs were then submerged in 100% acetone for 1 week to dehydrate the muscles and then in 80% xylene for an additional week, creating a lipophilic effect to dissect the adipose tissue, which is an innovative step in the dissection technique.

Boiling

According to traditional dissection techniques, the hearts should be boiled empirically according to size until malleable tissue is achieved by denaturing of the connective tissue. The time required varies from 10 minutes to 2 hours,⁸ making it difficult to estimate the time without experience. To standardize boiling and to perform objective dissection, larger bovine hearts were preferred. The boiling time was determined by measuring a 38% loss of heart mass, achieving adequate muscle malleability; later the same loss was obtained in porcine and human hearts, achieving malleability. The percent loss is calculated by weighing the hearts before and during boiling until 38% of the initial weight has been lost (Figure 1A-C).

Dissection of the Myocardium

To aid comprehension, please refer to the Figures and [Video in the supplementary data](#).

The adipose tissue was dissected in the anterior interventricular, posterior interventricular, and atrioventricular (AV) sulci, as well as in the circulatory system.

Detachment of the Atria

Manual pressure is exerted against the AV sulcus until the atria are penetrated, pulling them upward until they are detached.

Length of the Pulmonary Artery and Aorta

The pulmonary artery and aorta are sectioned at 3 to 5 cm above their origin to handle the heart more easily, taking note of the separation between the pulmonary artery and the aorta. This is used as a reference to begin dissecting the BL in its right segment (RS).⁸

Basal Loop

The basal loop is composed of the RS and the left segment (LS). The free wall of the right ventricle (RV) is formed by the RS, and the free wall of the left ventricle (LV), by the LS; the left marginal artery defines the path of the LS until it reaches the base of the aorta.

Separation of the Large Vessels

The thumb is used to exert traction until the pulmonary artery is separated from the aorta, arriving to the fibrous annulus of the tricuspid valve, which is sectioned. This is facilitated by placing a finger inside the aorta to hold the heart and limit its motion.

Dissection of the Right Segment

Pressure should be exerted over the entire length of the anterior interventricular sulcus until entering the RV. The septomarginal trabecula is then located and separated from the septal wall to obtain a muscle covering of the RS.

Main Reference Points

The dissection then identifies the inferior surface of the RV, which corresponds externally to the posterior interventricular sulcus. At the bottom of the cavity, a dihedral angle of 90° is formed where the BL intersects the interventricular septum (IVS), an anatomic correlation previously described by Torrent-Guasp^{8–10} and retaken to find the laminar plane of the dihedral angle that releases the LS.

Dissection of the Left Segment

Using the index finger or thumb, the inferior surface of the RV or posterior interventricular sulcus is pressed on the outside. Here, the dihedral angle is formed and is detached until detecting a change in fibers from endocardial to myocardial in the horizontal direction. To release it, lateral traction is exerted on the descending segment (DS) with both thumbs. Because the fibers are thinner in the human heart, traction can be exerted with a grooved director in the same direction. Once the muscle plane is found, it should be followed to the LV base at its posterior portion. Care should be taken with the fibers, as they have an ascending and oblique direction following the course of the left marginal artery until its origin, where the left fibrous trigone is inserted and must be cleaved.

Sectioning of the Fibrous Trigones

The fibrous trigones connect the aorta to the base of the LV at the right and left ends. Once the BL is completely dissected, the left trigone should be cleaved, and when the dissection of the apical loop is started, the right trigone can be sectioned and the aorta detached.

Apical Loop

The AL forms the LV and has 2 segments: an endocardial segment (DS) and an epicardial ascending segment (AS). Both close the chamber helically and when crossing over each other, create a right angle and form the IVS.¹⁰

Dissection of the Descending Segment

After the BL is fully dissected, there is a change in muscle fibers toward the endocardium, where the index finger is inserted, following their path and dissecting the planes.

Identification of the 90° Angle

At the dihedral angle in the RV and the start of the LS of the BL with the posterior interventricular sulcus, the muscle fibers intersect at a 90° angle between the DS and the septal papillary muscle of the RV. The fibers crossing horizontally (subendocardium) correspond to the DS, and the fibers in the vertical direction (subepicardium) correspond to the AS.

Dissection of the Ascending Segment and Detachment of the Aorta

Once the 90° intersection is located, pressure is exerted with the thumb or index finger (according to the dissector) between the horizontal and transversal planes. The aim is to find a change in the direction of muscle fibers to release the AS up to the LV base by sectioning the right fibrous trigone. Once the 2 muscle planes are separated, it is necessary to return to the place where the LS becomes the DS, to insert the index finger to dissect the path of the DS and AS completely, and to detach the aorta attached to the AS.

Opening of the Myocardial Band

The above step is important because if performed properly, it will only be necessary to follow the natural direction of the epicardial fibers until they enter the endocardium of the LV from its posterior aspect, the reference point of the posterior papillary muscle (PPM), which is the border where the AS starts. The mitral annulus is sectioned, and the LV is unrolled to obtain the helical myocardial band.

Echocardiographic Views

Once the myocardium of the hearts was completely dissected, the segments were identified by color coding (BL: RS, blue; LS, red; AL: DS, yellow; AS, green). The hearts were rolled back into their original position without the atria to obtain the echocardiography slices according to the views to be correlated (long-axis, short-axis, and apical 4-chamber). Echocardiographic images were obtained from healthy adult patients; the velocity vector images were taken from an undiseased fetal heart of 40.2 weeks.

RESULTS

Standardization

Differences in heart weight, heart size, and boiling method had no relevant effects, and adequate malleability for dissecting was achieved in all hearts with 38% loss of mass. By describing and specifying the technique, it should now be easier to dissect the myocardium than with the original procedure. No anatomic differences between human, bovine, and porcine hearts were found in the band. Prior fixation of human hearts hampers their dissection compared with fresh hearts.

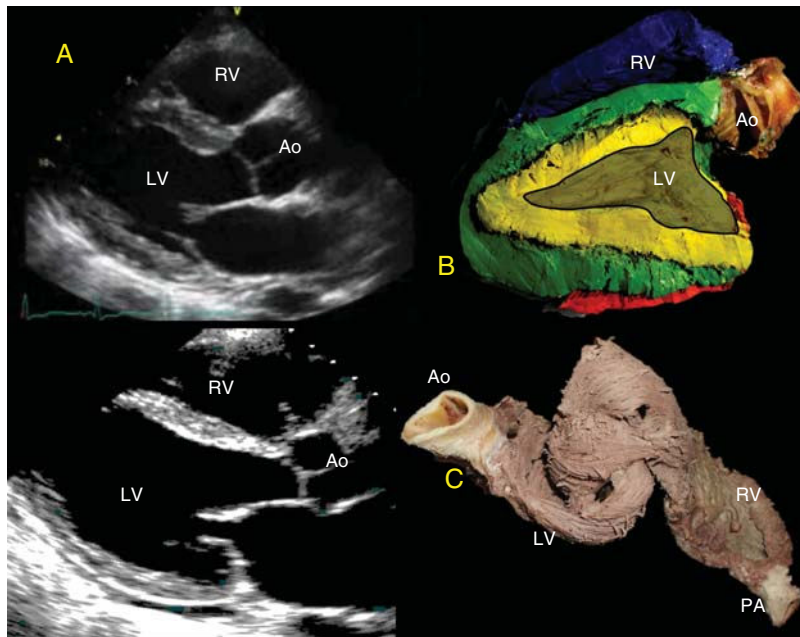


Figure 2. A, Parasternal long-axis view. B, correlation with the long-axis, showing the IVS with the double muscle plane and the free wall of the LV; the DS (green) surrounds the AS (yellow). C, partially rolled up bovine heart. Ao, aorta; AS, ascending segment; DS, descending segment; IVS, interventricular septum; LV, left ventricle; PA, pulmonary artery; RV, right ventricle.

Topographic Correlation: Echocardiography

Parasternal Long-axis

The free wall of the RV is formed in its entirety by the RS of the BL (blue); its continuity to the LS (red) contributes a small portion in the posterobasal region of the free wall of the RV covering the AS. The IVS is formed in its entirety by the 2 segments, the DS and the AS (yellow and green). The base of the LV shows the 4 segments of the band, whereas only the DS and AS are in the middle portion and the apex (Figure 2). It is important to consider that the AS begins

after the PPM and, therefore, visualization at the halfway point does not allow the AS to be seen.

Parasternal Short-axis

The RS (blue) forms the entire free wall of the RV, the LS (red) is smaller and covers the posterolateral portion of the LV; it is interesting to note that the DS occupies most of the LV, rotates 360°, and closes the LV in all sections (Figure 3). However, depending on the height or depth of the slice, the segments provide

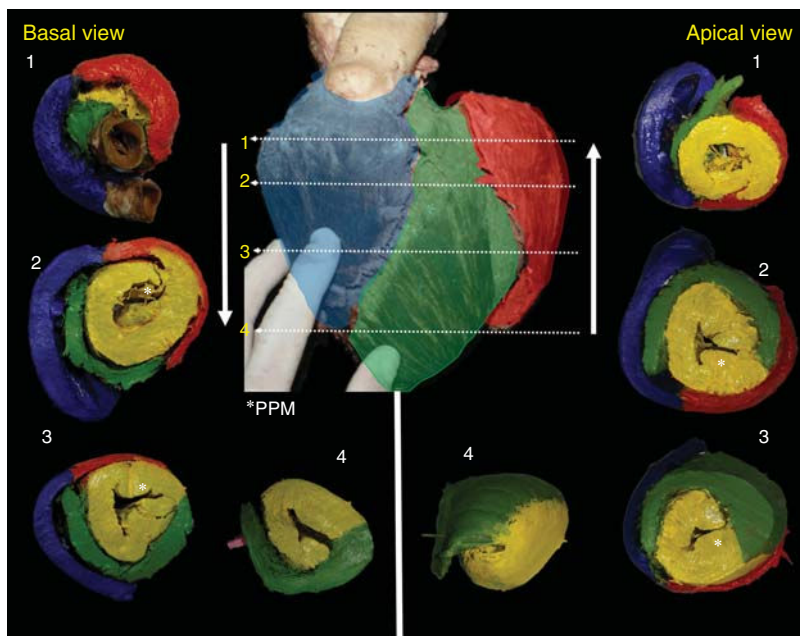


Figure 3. Correlated short-axis slices seen from the top to the apex and from the apex to the top. The numbers indicate the site of the slice location for each piece. Note that the DS (yellow) closes the LV completely and after PPM (*), originates the AS, which rotates 180° over its endocardial homologue. In the middle anterior view, the anterior descending artery divides the RS (blue) from the AS (green); the marginal artery marks the division between the LS (red) and the AS (green). AS, ascending segment; DS, descending segment; LS, left segment; LV, left ventricle; PPM, posterior papillary muscle; RS, right segment.

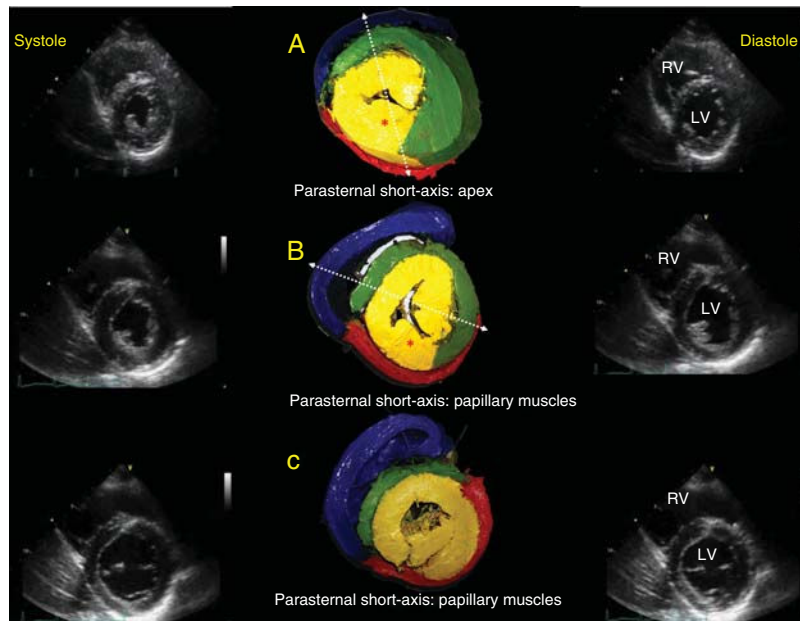


Figure 4. Echographic correlation with short-axis views in systole and diastole. Emphasis on 3 anatomic relationships: apical short-axis (A), papillary muscle short-axis (B), and mitral valve short-axis (C). The asterisk indicates the PPM. The dotted lines in A and B show that, according to the view angle used, the AS has a different appearance in the free wall of the LV; as the slice becomes more vertical, it passes more completely over the PPM, and as it becomes more oblique and passes through the anterior papillary muscle, the AS becomes more visible in the free wall of the LV and can be assessed. AS, ascending segment; LV, left ventricle; PPM, posterior papillary muscle; RV, right ventricle.

more or less to the anatomy (Figure 4). The PPM is followed by the AS, which rotates 180° and covers its endocardial homologue until reaching the posterior interventricular sulcus, where the 4 segments intersect (Figure 3 and Figure 4).

Apical 4-chamber

The LV endocardium will always be occupied by the DS (yellow). Depending on the echocardiographic depth, the AS

(green) appears in the lateral wall of the LV (Figure 5). The separation between the DS and the AS in the IVS is seen as a bright line in the standard ultrasound (Figures 5A, 5B, and 5D). When the PPM is observed, part of the AS is hard to visualize because this papillary muscle still forms part of the DS (yellow) (Figure 5B). In more superficial views toward the anterior aspect of the LV, it is possible to observe that the AS (green) surrounds the DS (yellow) (Figure 5C), which is important for evaluating the isovolumetric relaxation phase by radial/longitudinal deformation vectors (Figure 6).

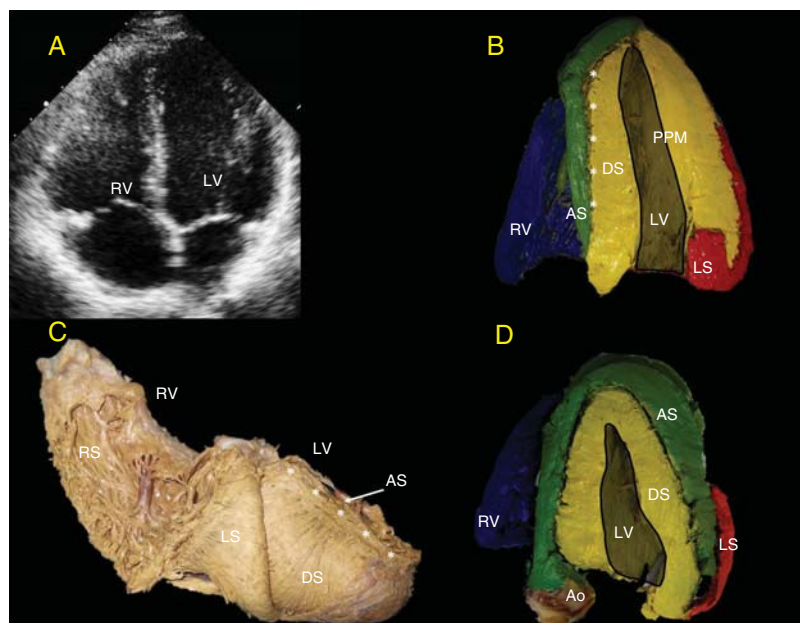


Figure 5. A, 4-chamber view. B, the bright echogenic line divides the septum into the DS and the AS (asterisks). C, human heart in right posterolateral view showing superimposition of the DS and AS over the septum that produces the bright echogenic line (asterisk). D, as the slice moves closer to the anterior aspect of the heart, the heart shows the AS more clearly in the free wall of the LV; as the slice move farther away and crosses more completely over the PPM, only the DS and LS will be seen in the free wall, as occurs in A above. Ao, aorta; AS, ascending segment; DS, descending segment; LS, left segment; LV, left ventricle; PPM, posterior papillary muscle; RS, right segment; RV, right ventricle.

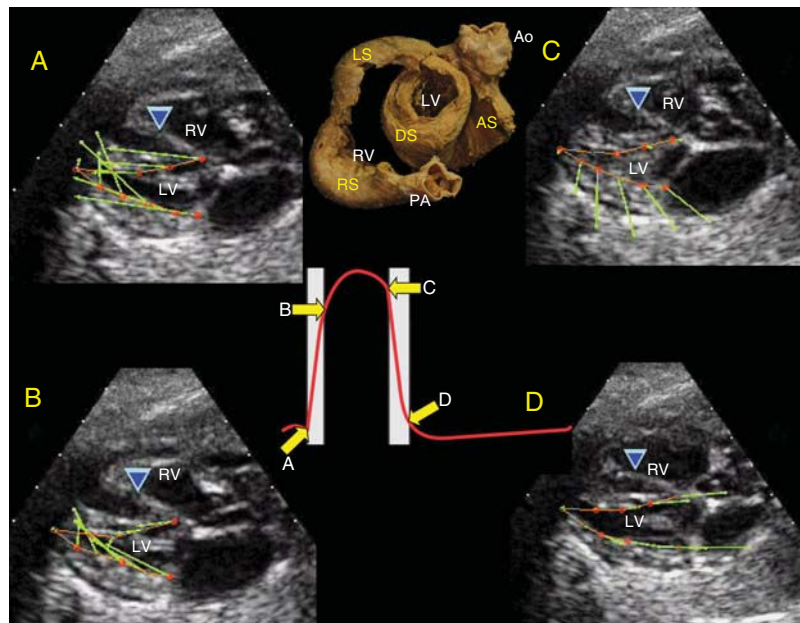


Figure 6. Four-chamber views and velocity vectors in 40.2-week fetal heart on ultrasound. A, velocity vectors (green arrows) from the LV base in the caudal direction during axial shortening motion. B, the vectors move toward the interior in the lateral wall and the upper portion of the IVS by DS contraction during ejection. C and D, start of the isovolumetric relaxation period in which the AS contracts, the velocity vectors in the lateral and outward direction in the cephalic direction, which leads to untwisting and axial elongation of the heart. Partially rolled up human heart. Wiggers diagram, showing velocity vector-related motion during the cardiac cycle. A, basal loop contraction. B, DS contraction. C, AS contraction, ventricular relaxation. Ao, aorta; AS, ascending segment; DS, descending segment; IVS, interventricular septum; LS, left segment; LV, left ventricle; PA, pulmonary artery; RS, right segment; RV, right ventricle.

Orientation of Subendocardial and Subepicardial Fibers

The muscle fibers rotate 180° at the transition from the LS to the DS and orient the subendocardial fibers at a 45° angle in a vertically oriented pattern toward the cardiac apex, and after the PPM, are reoriented at 45° to become subepicardial fibers with a predominantly oblique orientation, which creates the helicoid, conicity, and vortex of the apex.

DISCUSSION

Importance of Dissection

In his extensive research, Torrent-Guasp¹ identified the anatomy of the myocardium as a single band by using a manual dissection technique that he developed over more than 50 years of study. However, dissection is difficult, and reproducing it without adequate instructions does not lead to success. Torrent-Guasp^{6,8–10} provides the key points defining the cleavage planes to divide the myocardium; however, the empirical preparation he had mastered omits important details that would have allowed others to undertake the procedure. A lack of standardization and detailed instructions has led various authors to publish dissection techniques that do not completely unfold the band¹¹ or respect the segments in which it is divided.¹² The technique described herein is more specific and descriptive and indicates how to use Torrent-Guasp's anatomic references during manual dissection. Immersion in acetone is an innovative step that promotes tissue dehydration, and xylene has a lipophilic effect on fixed human adipose tissue. Gunther von Hagens and other authors^{13,14} have used hydrocarbons to dehydrate and eliminate tissue lipids. Another important contribution is the 38% loss of mass, which ensures the texture and malleability needed for manual myocardial dissection of any size of heart, including the human heart. This

parameter is not included in other studies and provides a more objective dissection technique.

Understanding the Anatomy

The helical arrangement of the fibers has been confirmed by tractography with no need to dissect the heart,^{15,16} which validates the dissection. A theoretical understanding of the anatomy of the heart is insufficient to develop more clinical applications of the concept, whereas familiarity with dissection provides a clearer understanding of the structural architecture in which myocardial fibers are distributed, applying the concept in surgery^{17,18} and imaging studies.^{2,19,20} The correlations morphologically reveal the distribution of the segments in the echocardiographic long-axis, short-axis, and 4-chamber views. The correlations exhibit further validity if they are sought intentionally and evaluated by strain, strain rate, and velocity vectors.

Echocardiogram-correlated Implications

Each segment correlated in this study represents already defined movements as well as mechanical actions that involve 6 movements during the cardiac cycle^{21–23} (Figure 6).

Systole:

1. Narrowing: decreases the transverse diameter; the BL and its 2 segments contract (isovolumetric contraction).
2. Twisting: DS contraction (rapid ejection).
3. Axial shortening: due to DS contraction, the base moves closer to the apex.

Diastole:

4. Axial elongation: AS contraction, producing an untwisting movement during isovolumetric relaxation.

5. Untwisting during isovolumetric relaxation.
6. Widening: attributed to chamber filling, BL rest, and the resulting clockwise rotation when the heart untwists.

During the scan, the angle between the DS and the AS appears to be crucial for efficient systolic function.²⁴ To assess the displacement angle of fibers during twisting and untwisting by speckle-tracking echocardiography or velocity vector imaging, the short-axis near the base or the middle portion of the LV²⁵ (Figures 4B and 4C) provide well-defined images of the 4 segments. A window near the apex only shows the AL components (DS, AS) (Figure 3, #4). The 4-chamber view shows a bright echogenic line in the IVS that marks the separation between the DS and the AS²⁶ (Figure 5).

Clinical Context

The systolic component of the DS and the diastolic component of the AS (Figures 6B and 6C) were evaluated in hypertensive and healthy patients, finding that normal patients had similar peak twist velocity in systole of 1.9 ± 0.2 cm/s, whereas hypertensive patients showed a faster deformation velocity of 2.3 ± 0.2 cm/s. The ventricular untwist velocity during the isovolumetric relaxation phase was measured at 1.7 ± 0.1 cm/s in healthy individuals, but was lower in hypertensive patients, 1.1 ± 0.1 cm/s.²⁷ The generation of lower contractile strength by the AS could morphologically explain the development of early diastolic dysfunction, which would enhance ultrasound diagnosis in the future.

An understanding of the topographic anatomy of the band in the echocardiogram could provide a deformation velocity standard for each segment in healthy individuals and unwell patients to be included as a clinical parameter for use in stratifying and obtaining prognoses in diseases, such as subclinical systolic and diastolic dysfunction in metabolic syndrome,^{28,29} and predicting cardiotoxicity in cancer patients.^{30,31} Following an acute myocardial infarction, some patients experience intramyocardial dissecting hematomas and ruptures that appear on ultrasound to follow the helical architectural pattern, dissecting the apex in the endomyocardium and IVS in half, as shown; in others there is hemorrhagic dissection where the 4 segments connect, and these cases tend to progress with dissection of the segments of the band.³²

Controversies

Several models have been proposed for the architecture of myocardial fibers, such as that of cardiac mesh, in which the myocytes are arranged at different depths in the longitudinal and radial courses.³³ However, the helical model has helped to explain the dynamics of contraction during the cardiac cycle more efficiently.³⁴ In parallel, it has been determined that the loss of LV twisting is the earliest sign of heart failure, which can be clarified by studying contraction using the anatomic correlation described. It has recently been found that electric activation extends radially from the DS to the AS at the intersection of the helical segments in the IVS, while simultaneous and opposite activation of the proximal and distal AS begins, confirming the presence of circumferential fibers not described in the helical model.³⁵

CONCLUSIONS

A standard dissection technique can be used to successfully dissect helical fibers in human hearts as well as in hearts from

other species, while retaining the segmentation of the myocardium. No anatomic differences were found between bovine, porcine, and human hearts. Echographic correlation identifies where each segment of the band is found in the long-axis, short-axis, and apical 4-chamber views, essential for analyzing myocardial function, which is the only distinctive feature for determining structure credibility. Echocardiography is useful to identify the various segments of the helical myocardium and its deformation-based performance.

ACKNOWLEDGMENTS

I would like to thank Dr C.M. Alberto Sosa Olavarría for providing the echocardiography images for this correlation and Dr Cristóbal Rubén Villavicencio Nava for providing the laboratory facilities during his coordination.

CONFLICTS OF INTEREST

None declared.

WHAT IS KNOWN ABOUT THE TOPIC?

- The anatomy of the heart helically divided into 4 segments is known to explain cardiac mechanics during the cardiac cycle in 6 defined movements; therefore, the shape of the heart explains its motion.
- Some intramyocardial hematomas and myocardial ruptures follow the path of the helical segments.
- Familiarity with the topographic anatomy of the heart is extremely useful in diagnostic imaging.

WHAT DOES THIS STUDY ADD?

- A standard dissection process is described. To avoid errors during dissection, video material is included to provide a step-by-step explanation of the most important movements in human, bovine, and porcine hearts.
- This is an improved technique for teaching and research. Close anatomic correlation is shown with the echocardiographic views most commonly used; hence, a segment of interest can be assessed in more detail, based on a clear understanding of the view where it can be found, leading to a new perspective for assessing structural disease.

APPENDIX. SUPPLEMENTARY DATA

Supplementary data associated with this article can be found in the online version, at <https://doi.org/10.1016/j.rec.2018.10.016>.

REFERENCES

1. Torrent-Guasp F. *El músculo cardíaco*. Madrid: March FJ; 1972.
2. Buckberg GD, Castellá M, Gharib M, Saleh S. Active myocyte shortening during the 'isovolumetric relaxation' phase of diastole is responsible for ventricular suction; 'systolic ventricular filling'. *Eur J Cardiothorac Surg*. 2006;29(Suppl 1):S98–S106.
3. Cosín Aguilar JA, Hernández Martínez A, Tuzón Segarra MT, Agüero Ramón-Llin J, Torrent-Guasp F. Estudio experimental de la llamada fase de relajación isovolumétrica del ventrículo izquierdo. *Rev Esp Cardiol*. 2009;62:392–399.

4. Carreras F, García-Barnes J, Gil D, et al. Left ventricular torsion and longitudinal shortening: two fundamental components of myocardial mechanics assessed by tagged cine-MRI in normal subjects. *Int J Cardiovasc Imaging*. 2012;28:273–284.
5. Nasiraei-Moghaddam A, Gharib M. Evidence for the existence of a functional helical myocardial band. *Am J Physiol Heart Circ Physiol*. 2009;296:H127–H131.
6. Torrent-Guasp F. Estructura y función del corazón. *Rev Esp Cardiol*. 1998;51:91–102.
7. Torrent-Guasp F, Buckberg GD, Clemente C, Cox JL, Coghlan HC, Gharib M. The structure and function of the helical heart and its buttress wrapping. I. The normal macroscopic structure of the heart. *Semin Thorac Cardiovasc Surg*. 2001;13:301–319.
8. Torrent-Guasp F. Ventricular myocardial band-form. Disponible en: <http://www.torrent-guasp.com/pages/vmb%20form.htm>. Consultado 10 Oct 2018.
9. Kocica MJ, Corno AF, Carreras-Costa F, et al. The helical ventricular myocardial band: global, three-dimensional, functional architecture of the ventricular myocardium. *Eur J Cardiothorac Surg*. 2006;29(Suppl 1):S21–S40.
10. Torrent-Guasp F. Estructuración macroscópica del ventrículo izquierdo. (I) Mitad apéxica. *Rev Esp Cardiol*. 1972;25:68–81.
11. Salamanca DR, Bernal-García M, Castro ID. Disección experimental de la banda miocárdica ventricular. *Rev Investig Salud Univ Boyacá*. 2015;2:148–161.
12. Trainini JC, Herreros J, Elenchwaj B, et al. Disección del miocardio. *Rev Argent Cardiol*. 2017;85:44–50.
13. Skalkos E, Williams G, Baptista CAC. The E12 technique as an accessory tool for the study of myocardial fiber structure analysis in MRI. *J Int Soc Plastination*. 1999;14:18–21.
14. Arias López LA. Exploración de la técnica de plastinación en la preparación de modelos anatómicos como material docente para la enseñanza de la Morfología Humana en la Universidad Nacional de Colombia, sede Bogotá. Bogotá: Universidad Nacional de Colombia; 2012. Available at: <http://www.bdigital.unal.edu.co/8938/1/05599078.2012.pdf>. Accessed 10 Oct 2018.
15. Lombaert H, Peyrat JM, Croisille P, et al. Human atlas of the cardiac fiber architecture: study on a healthy population. *IEEE Trans Med Imaging*. 2012;31:1436–1447.
16. Poveda F, Gil D, Martí E, Andaluz A, Ballester M, Carreras F. Helical Structure of the Cardiac Ventricular Anatomy Assessed by Diffusion Tensor Magnetic Resonance Imaging With Multiresolution Tractography. *Rev Esp Cardiol*. 2013;66:782–790.
17. Torrent-Guasp F. La estructura de la pared ventricular y su proyección quirúrgica. *Cir Cardiovasc*. 1972;1:93–108.
18. Isomura T, Horii T, Suma H, Buckberg GD; RESTORE Group. Septal anterior ventricular exclusion operation (Pacopexy) for ischemic dilated cardiomyopathy. *Eur J Cardiothorac Surg*. 2006;29(Suppl 1):S245–S250.
19. Sosa Olavarria A, Pérez-Canto Chelliu G, Giugnide Schenone G, et al. Evaluación del rendimiento ventricular del corazón fetal en función de la banda miocárdica helicoidal. *Ultrasonografía Embrio-Fetal*. 2010;5:7–13.
20. Buckberg G, Mahajan A, Saleh S, Hoffman JI, Coghlan C. Structure and function relationships of the helical ventricular myocardial band. *J Thorac Cardiovasc Surg*. 2008;136:578–589.
21. Buckberg G, Hoffman JI, Mahajan A, Saleh S, Coghlan C. Cardiac mechanics revisited: The relationship of cardiac architecture to ventricular function. *Circulation*. 2008;118:2571–2587.
22. Buckberg G, Hoffman JI, Nanda NC, Coghlan C, Saleh S, Athanasuleas C. Ventricular torsion and untwisting: Further insights into mechanics and timing interdependence: A viewpoint. *Echocardiography*. 2011;28:782–804.
23. Buckberg GD, Hoffman JI, Coghlan HC, Nanda NC. Ventricular structure-function relations in health and disease: Part I. The normal heart. *Eur J Cardiothorac Surg*. 2015;47:587–601.
24. Sengupta PP, Tajik AJ, Chandrasekaran K, Khandheria BK. Twist mechanics of the left ventricle. *JACC Cardiovasc Imaging*. 2008;1:366–376.
25. Kocabay G, Muraru D, Peluso D, et al. Mecánica ventricular izquierda normal mediante ecocardiografía speckle tracking bidimensional. Valores de referencia para adultos sanos. *Rev Esp Cardiol*. 2014;67:651–658.
26. Hayabuchi Y, Sakata M, Kagami S. Assessment of the helical ventricular myocardial band using standard echocardiography. *Echocardiography*. 2015;32:310–318.
27. Vannan MA, Pedrizzetti G, Li P, et al. Effect of cardiac resynchronization therapy on longitudinal and circumferential left ventricular mechanics by velocity vector imaging: description and initial clinical application of a novel method using high-frame rate B-mode echocardiographic images. *Echocardiography*. 2005;22:826–830.
28. Cañón-Montañez W, Santos ABS, Lisandra, et al. La obesidad central es el componente clave en la asociación del síndrome metabólico con el deterioro del strain longitudinal global del ventrículo izquierdo. *Rev Esp Cardiol*. 2018;71:524–530.
29. Tadic M, Cuspidi C, Majstorovic A, et al. Does the metabolic syndrome impact left ventricular mechanics? A two-dimensional speckle tracking study. *J Hypertens*. 2014;32:1870–1878.
30. Stanton T, Leano R, Marwick TH. Prediction of all-cause mortality from global longitudinal speckle strain. *Circ Cardiovasc Imaging*. 2009;2:356–364.
31. López-Fernández T, Thavendiranathan P. Nuevas técnicas de imagen cardíaca en la detección precoz de cardiotoxicidad secundaria a tratamientos oncológicos. *Rev Esp Cardiol*. 2017;70:487–495.
32. Vargas-Barrón J, Antúnez Montes OY, Roldán FJ, et al. Myocardial rupture in acute myocardial infarction: mechanistic explanation based on the ventricular myocardial band hypothesis. *Rev Invest Clin*. 2015;67:318–322.
33. Anderson RH. Spatial orientation of the ventricular muscle band. *J Thorac Cardiovasc Surg*. 2002;124:1053.
34. Cosín Aguilar J, Hernández Martínez A. La disposición de las fibras miocárdicas en una banda condiciona la morfología y la función del corazón. *Rev Esp Cardiol*. 2013;66:768–770.
35. Trainini J, Elenchwaj B, López-Cabanillas N, Herreros J, Lago N. Electrophysiological bases of torsion and suction in the continuous cardiac band model. *Anat Physiol*. 2015;54:001.